The Astronomical Journal, 150:70 (8pp), 2015 September doi:10.1088/0004-6256/150/3/70

PHOTOMETRIC STUDY AND PERIOD ANALYSIS OF THE CONTACT BINARY XZ LEONIS

Chang Qing Luo, Xiao Bin Zhang, Licai Deng, Kun Wang, and Yangping Luo
Key Laboratory of Optical Astronomy, National Astronomical Observatories, Chinese Academy of Sciences, Beijing 100012, China; changqingluo@bao.ac.cn
Received 2014 November 17; accepted 2015 June 17; published 2015 August 12

ABSTRACT

We present multi-color CCD photometry of the neglected contact binary XZ Leo. Completely covered *VRI* band light curves and four times of minimum light were obtained. Combining the photometric and previously published radial-velocity data, a revised photometric analysis was carried out for the binary system by applying the Wilson–Devinney code. With a hot spot placed on the massive primary component near the neck region of the common envelope, the light curves were satisfactorily modeled. The photometric solution combined with the radial-velocity solution reveals that XZ Leo is an A-type contact binary with a degree of contact of 24(±1)%. The absolute parameters of the components were determined to be $M_1 = 1.74(\pm0.06)M_\odot$, $M_2 = 0.61(\pm0.02)M_\odot$, $R_1 = 1.69(\pm0.01)R_\odot$, $R_2 = 1.07(\pm0.01)R_\odot$, $L_1 = 6.73(\pm0.08)\ L_\odot$, and $L_2 = 2.40(\pm0.04)L_\odot$. Based on all the available data, the long-term orbital period behavior of the system was investigated. It indicates that the binary system was undergoing a continuous orbital period increase in the past three decades with a rate of $dP/dt = +6.12 \times 10^{-8}$ days yr^{-1}, which suggests a probable mass transfer from the secondary to the primary component at a rate of $dM/dt = 3.92 \times 10^{-8} M_\odot$ yr^{-1}. The binary system is expected to evolve into the broken-contact stage in 1.56×10^6 years. This could be evidence supporting the thermal relaxation oscillation theory.

Key words: binaries: close – binaries: eclipsing – stars: evolution – stars: individual (XZ Leo)

1. INTRODUCTION

The light variation of XZ Leo (BD + 17°2165, GSC 01412-01030) was discovered by Hoffmeister (1934). Prichodko (1947) pointed out that this system is a W UMa-type contact binary. The first photoelectric light curves of XZ Leo were obtained by Hoffmann (1984) and were analyzed by Niarchos et al. (1994). They noted that the light curves presented asymmetries between the first and second light maxima and that the second maximum was slightly displaced to phase 0.76. They suggested that there might be two hot spots on both components located near the neck region of the common envelope. Subsequently, Rucinski & Lu (1999) obtained the radial-velocity curves of this system. The radial-velocity solution revealed a mass ratio of 0.348 (±0.029) for the binary system based on mass-centered sinusoids. About 10 years later complete *BVRI* light curves were obtained by Lee et al. (2006). They claimed a blue third light and a hot spot near the neck of the primary component in their model. The solutions suggested that the system is a deep contact binary ($f = 33.6\%$) with a small difference in temperature of $\triangle(T_1 - T_2) = 126$ K. Combined with the radial-velocity curves (Rucinski & Lu 1999), they determined the absolute parameters of XZ Leo as follows: $M_1 = 1.84M_\odot$, $M_2 = 0.63M_\odot$, $R_1 = 1.75R_\odot$, $R_2 = 1.10R_\odot$, $L_1 = 7.19L_\odot$, and $L_2 = 2.66L_\odot$. They also investigated all minimum light times to find the period increase at a rate of $dP/dt = +8.20 \times 10^{-8}$ days yr^{-1} for XZ Leo following Qian (2001a). They suggested that the continuous period increase of XZ Leo could be due to mass transfer from the secondary to the primary component and indicate that this system was undergoing an orbital expanding stage of thermal relaxation oscillation (TRO) cycles, as suggested by Qian (2001b). Therefore XZ Leo is a potentially key example as predicted by TRO theory, but there have been very few analyses of this system even though it has been known for many decades.

Therefore, we have carried out new photometric observations of the binary. We present multi-color CCD light curves in the *V*, *R*, and *I* bands and analyze the light curves with the Wilson–Devinney (W–D) code. The new photometric solutions of the system are derived and the absolute parameters are determined by combining spectroscopic and photometric solutions. Moreover, the variations in the orbital period of XZ Leo are analyzed. Period investigations are important in close binary studies, because they can not only provide information about some important physical processes (mass transfer, magnetic activity cycles), but also can give us a hint of the evolutionary stage of the binaries. To obtain an accurate period and period changes, long timespan data sets and precise times of minimum light data are important and necessary. Here, we collect all available original data of XZ Leo to obtain reliable results. Finally, based on the period changes and the photometric solutions of XZ Leo, the geometric structure and evolutionary stage of this system are discussed.

2. PHOTOMETRIC OBSERVATIONS

New CCD photometric observations of XZ Leo in the *V*, *R*, and *I* bands were made on three nights in 2014 (February 24 and 27 and March 9) with the 85 cm reflecting telescope at Xinglong station of the National Astronomical Observatory, Chinese Academy of Sciences (NAOC). A 1024 × 1024 PI CCD camera and a standard Johnson–Cousins–Bessel multi-color filter system were used during the observation (Zhou et al. 2009). The effective field of view is 16.′5 × 16.′5. A total of 2110 individual observations were obtained in the three bandpasses (735 in *V*, 732 in *R*, and 643 in *I*), which covered a timespan of about 24 hr. The twilight sky flat, bias, and dark frames were taken on each observing day, which were first

Table 1
Coordinates of XZ Leo and the Comparison and Check Stars

Target	Names	α2000	δ2000
Variable star(V)	XZ Leo	$10^h\ 02^m\ 34^s.19$	$+17^0\ 02'\ 47''.15$
The comparison star(C)	TYC 1412-247-1	$10^h\ 02^m\ 07^s.11$	$+16^0\ 59'\ 21''.28$
The check star(K)	BD+17 2163a	$10^h\ 02^m\ 20^s.20$	$+17^0\ 04'\ 12''.65$

processed with the standard routines of CCDPROC in the IRAF package. Then, the instrumental magnitudes of stars detected in the program field were obtained using PHOT of the aperture photometry package of IRAF. A star near the variable star was chosen as the comparison star (TYC 1412-247-1), which has a brightness and color similar to that of the variable star. Another star in the same field of view was selected as the check star (BD+17 2163a, GSC 01412-00423). The differential magnitudes of these stars were extracted in each frame. The corresponding coordinates of XZ Leo and the comparison and check stars are shown in Table 1. Complete light curves in the *V*, *R*, and *I* bands are displayed in Figure 1 with open circles, where phases were computed using a period of 0.487739 days. This period is reconfirmed with the new data in this paper.

As shown in Figure 1, the observational light curves with open circles are typical EW-type light curves where the depths of both light minima are nearly the same. The light curves do not show O'Connell effects (different heights of the two light maxima) of unequal light levels at the quadratures beyond the limits of the observational error of about ± 0.01 mag, but maxima I (phase = 0.25) and maxima II (phase = 0.75) of the light curves are displaced to around phases 0.24 and 0.76, respectively, which are shown in Figure 2. The solid line is maxima I at phase = 0.25 and maxima II at phase = 0.75 (upper panel), and the dotted line are phases at 0.24 and 0.76 (lower panel). These very same displacements are also found by Niarchos et al. (1994) in the Hoffmann (1984) light curve as well as in the Lee et al. (2006) light curves. That means this displacement of the maxima is a long-term effect probably indicative of a long-term asymmetry in the system. In our observations, a total of four eclipses of the contact binary XZ Leo were covered, including two primary and two secondary ones. By applying the K-W method (Kwee & van Woerden 1956), the epochs of minimum light with mean values of the *V*, *R*, and *I* filters were determined as given in Table 2.

3. PHOTOMETRIC SOLUTIONS WITH THE W–D METHOD

Combining the photometric and radial-velocity data, the light curves in the *V*, *R*, and *I* bands were analyzed using the W–D program (Wilson & Devinney 1971; Wilson 1979, 1990, 1994; Wilson & van Hamme 2003). We also assumed an effective temperature to be $T1 = 7160$ K for the primary component (the star eclipsed at primary minimum), which was averaged from tables in Harmanec (1988) and Flower (1996) corresponding to the spectral type A8V by the spectroscopy and color index in the Hipparcos and Tycho Catalogs (Lee et al. 2006). The gravity-darkening coefficients $g1 = g2 = 1.0$ (Lucy 1967) and the bolometric albedos $A1 = A2 = 1.0$ (Rucinski 1969) were used because each component should have a radiative envelope or at most a shallow convective atmosphere (Lee et al. 2006). The initial mass ratio q was fixed to the spectroscopic mass ratio $q = 0.348(\pm 0.029)$ obtained by Rucinski & Lu (1999). A nonlinear limb-darkening law with a

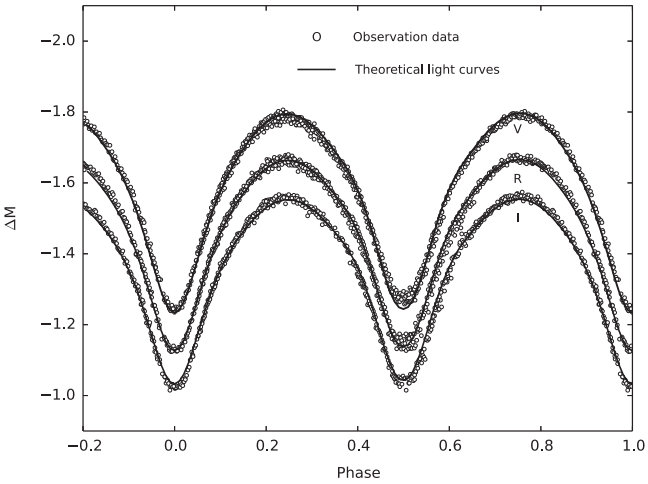

Figure 1. CCD photometric light curves in the *V*, *R*, and *I* bands obtained using the 85 cm telescope at NAOC on 2014 February 24 and 27 and March 9. Open circles denote the observational data in the *V*, *R*, and *I* bands. The solid line represents the theoretical light curves calculated using the W–D method discussed in Section 3.

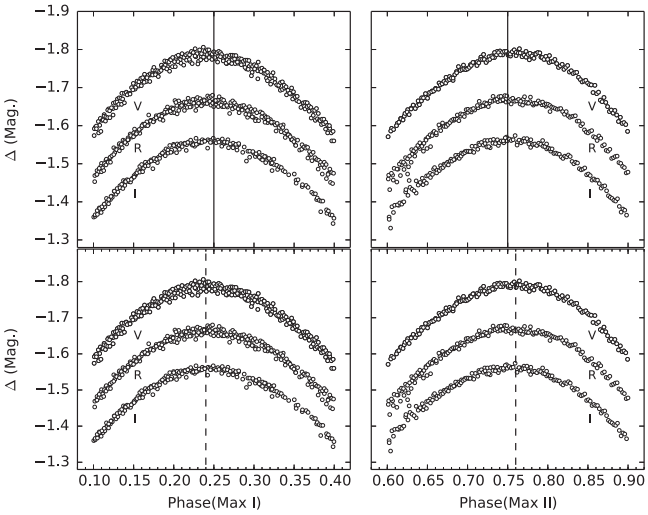

Figure 2. Maxima I and maxima II of the light curves. The solid lines in the top panels represent maxima I at phase = 0.25 and maxima II at phase = 0.75. The dotted lines in the bottom panels show the displaced maxima at phases 0.24P and 0.76P, respectively.

Table 2
New Times of Minimum Light for XZ Leo

HJD	Error	Type	Filter
2456713.0162	0.0001	I	*VRI*
2456713.2607	0.0001	II	*VRI*
2456716.1867	0.0001	II	*VRI*
2456726.1872	0.0002	I	*VRI*

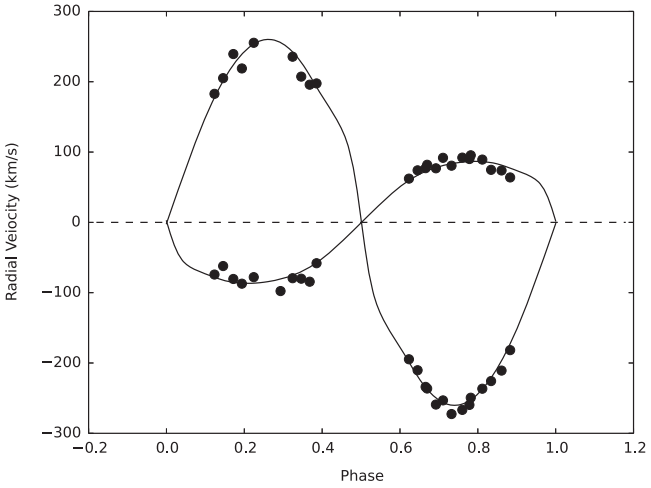

Figure 3. Radial-velocity curves of XZ Leo. The solid circles are the observational data (Rucinski & Lu 1999). The continuous curves are the theoretical synthesis including proximity effects.

logarithmic form was applied in the light-curves synthesis. The initial bolometric (X_1, X_2, Y_1, Y_2) and monochromatic limb-darkening coefficients (x_1, x_2, y_1, y_2,) of the components were taken from van Hamme (1993) and are listed in Table 3. The adjustable parameters are as follows: mass ratio, q; the inclination, i; the mean temperature of star 2, $T2$; the monochromatic luminosity of star 1, L_{1V}, L_{1R}, and L_{1I}; and the dimensionless potentials of star 1 and star 2 ($\Omega_1 = \Omega_2$ for mode 3).

As we discussed in the above section, the light curves of XZ Leo show light maxima displacement. Initially, when no other physical processes are added into the binary model, we cannot obtain a satisfactory fitting of the light curves. In order to solve this problem, a spot model was introduced. Since the displacement of the light maxima was noted in all the light curves obtained by Hoffmann (1984), Lee et al. (2006) and the present observations, it seems to be a long-lived phenomenon, which could not be caused by a cool spot related to magnetic activity. Qian (2001a) and Lee et al. (2006) found that the orbital period of XZ Leo was continuously increasing, suggesting probable mass transfer from the less massive secondary to the primary component. There are four spot parameters for each spot in the W–D program: the spot temperature ($T_s = T_d/T_0$; T_s is the ratio between the spot temperature T_d and the photosphere surface temperature T_0 of the star), the spot angular radius (r_s) in radians, the co-latitude of the spot center (θ) in degrees, and the longitude of the spot center (ϕ) in degrees. The preliminary spot longitude could be found approximately using the phases of spot distortion in the light curves. The other three parameters were calculated by fitting the theoretical light curves based on the observational data. Finally, the best fitting photometric solutions were obtained with a hot spot. The observed data (marked with open circles) and the theoretical light curves (marked with solid lines) are shown in Figure 1. The results and the parameters of the hot spot are shown in Table 3. The synthetic radial velocity curves are given in Figure 3. The corresponding geometric structure of the system with the hot spot is plotted in Figure 4. The hot spot is located on the primary star near the neck region of the common envelope.

Table 3
Photometric Solutions of Contact Binary XZ Leo

Parameters	Best-fit Value(Model 1)		
	Primary		Secondary
$g1 = g2$ (degree)		1.0	
$A1 = A2$ (degree)		1.0	
X_{bolo}	0.642		0.641
Y_{bolo}	0.259		0.253
x_V	0.680		0.688
y_V	0.297		0.290
x_R	0.582		0.592
y_R	0.295		0.291
x_I	0.490		0.501
y_I	0.277		0.275
i (degree)		77.89(12)	
$q = M_2/M_1$		0.346(16)	
T(K)	7160		6981(12)
Ω	2.517(2)		2.517(2)
$L_1/(L_1 + L_2)_V$		0.748(1)	
$L_1/(L_1 + L_2)_R$		0.738(2)	
$L_1/(L_1 + L_2)_I$		0.734(2)	
r(pole)	0.4541(4)		0.2821(4)
r(side)	0.4889(6)		0.2954(6)
r(back)	0.5185(7)		0.3366(9)
Latitude$_{spot}$ (degree)		89.9(2)	
Longitude$_{spot}$ (degree)		5.9(5)	
Radius$_{spot}$ (degree)		17.1(1)	
T_{spot}/T_2		1.079(5)	
f(%)		24(1)	

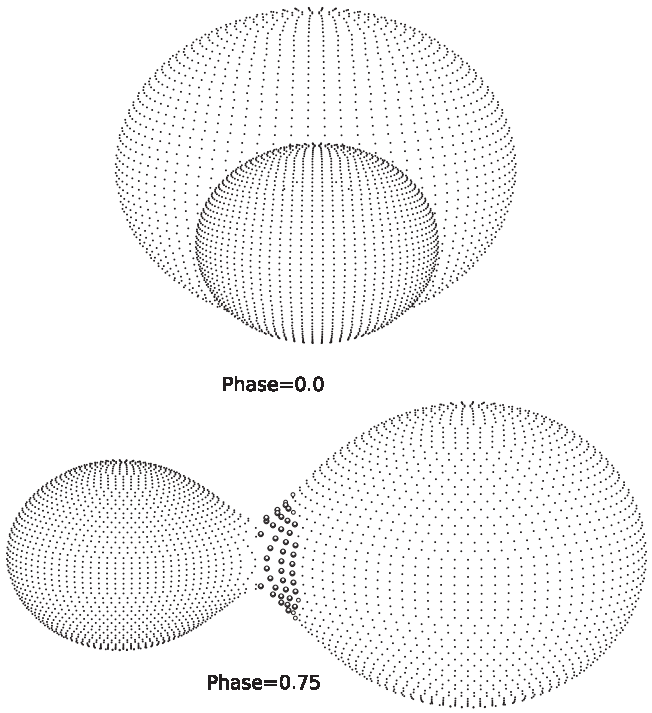

Figure 4. Geometrical configuration and the spot distribution of XZ Leo.

4. ORBITAL PERIOD VARIATIONS OF XZ LEO

In order to investigate the orbital period variations of XZ Leo, all available times of minimum light were collected from

Table 4
Photoelectric (Pe) and CCD Times of Minimum Light for XZ Leo

Epoch 2400000+	Type	Method	Epoch	*O–C*	References
45025.3580	p	Pe	−23990.0	0.0091	Hoffmann (1983)
45025.5950	s	Pe	−23989.5	0.0022	Hoffmann (1983)
45044.3710	p	Pe	−23951.0	0.0003	Braune & Mundry (1982)
45055.3475	s	Pe	−23928.5	0.0027	Braune & Mundry (1982)
45732.8154	s	Pe	−22539.5	0.0026	*O–C* gateway[a]
45732.8145	s	Pe	−22539.5	0.0017	Faulkner (1986)
45779.3971	p	Pe	−22444.0	0.0053	Hubscher & Mundry (1984)
46079.8407	p	Pe	−21828.0	0.0024	Faulkner (1986)
46177.3872	p	Pe	−21628.0	0.0013	Hubscher et al. (1985)
46910.4568	p	Pe	−20125.0	0.0008	Keskin & Pohl (1989)
47609.3834	p	Pe	−18692.0	−0.0010	Wunder et al. (1992)
47609.3852	p	Pe	−18692.0	0.0008	Hubscher et al. (1989)
47609.3858	p	Pe	−18692.0	0.0014	Hubscher et al. (1989)
47609.3859	p	Pe	−18692.0	0.0015	Hubscher et al. (1989)
47609.3865	p	Pe	−18692.0	0.0021	Hubscher et al. (1989)
47612.3100	p	Pe	−18686.0	−0.0008	Hubscher et al. (1989)
47612.3106	p	Pe	−18686.0	−0.0002	Hubscher et al. (1989)
47612.3113	p	Pe	−18686.0	−0.0001	Hubscher et al. (1989)
47613.5278	s	Pe	−18686.0	0.0005	Hubscher et al. (1989)
47613.5294	s	Pe	−18683.5	−0.0024	Hubscher et al. (1989)
47614.5054	s	Pe	−18683.5	−0.0008	Hubscher et al. (1989)
47614.5059	s	Pe	−18681.5	−0.0003	Hubscher et al. (1989)
47614.5064	s	Pe	−18681.5	0.0002	Hubscher et al. (1989)
47616.4579	s	Pe	−18681.5	0.0007	Hubscher et al. (1989)
47616.4582	s	Pe	−18677.5	0.0013	Hubscher et al. (1989)
47616.4585	s	Pe	−18677.5	0.0016	Hubscher et al. (1989)
48500.4840	p	Pe	−18677.5	0.0019	*O–C* gateway[a]
48680.4545	p	CCD	−16865.0	0.0024	Diethelm (1992)
48733.3760	s	CCD	−16496.0	−0.0024	Hubscher et al. (1992)
48733.3800	s	CCD	−16387.5	−0.0004	Hubscher et al. (1992)
49004.5572	s	Pe	−16387.5	0.0036	Hubscher et al. (1993)
49400.3578	p	Pe	−15831.5	−0.0015	Hubscher et al. (1994)
49400.3579	p	Pe	−15020.0	−0.0002	Hubscher et al. (1994)
49401.3321	p	Pe	−15020.0	−0.0001	Hubscher et al. (1994)
49439.3759	p	CCD	−15018.0	−0.0014	Hubscher et al. (1994)
49439.3762	p	Pe	−14940.0	−0.0012	Hubscher et al. (1994)
49439.3763	p	Pe	−14940.0	−0.0009	Hubscher et al. (1994)
49439.3766	p	Pe	−14940.0	−0.0008	Hubscher et al. (1994)
49756.4048	p	Pe	−14940.0	−0.0005	Agerer & Hubscher (1996)
49756.4050	p	Pe	−14290.0	−0.0019	Agerer & Hubscher (1996)
49756.4051	p	Pe	−14290.0	−0.0017	Agerer & Hubscher (1996)
49756.4053	p	Pe	−14290.0	−0.0016	Agerer & Hubscher (1996)
49776.4021	p	Pe	−14290.0	−0.0014	Diethelm (1995)
50137.3277	p	Pe	−14249.0	−0.0019	Agerer & Hubscher (1996)
50137.5702	s	Pe	−13509.0	−0.0023	Agerer & Hubscher (1996)
50137.5708	s	Pe	−13508.5	−0.0037	Agerer & Hubscher (1996)
50137.5709	s	Pe	−13508.5	−0.0031	Agerer & Hubscher (1996)
50137.5715	s	Pe	−13508.5	−0.0030	Agerer & Hubscher (1996)
50175.3742	p	CCD	−13508.5	−0.0024	Agerer & Hubscher (1997)
50195.3700	p	CCD	−13431.0	0.0006	*O–C* gateway[a]
51163.5287	p	CCD	−13390.0	−0.0008	Agerer & Hubscher (1999)
51222.5464	p	CCD	−11405.0	−0.0019	Agerer & Hubscher (2000)
51256.4434	s	CCD	−11284.0	−0.0005	Agerer & Hubscher (2000)
51276.1930	p	CCD	−11214.5	−0.0013	*O–C* gateway[a]
51629.8070	p	CCD	−11174.0	−0.0050	Nelson (2001)
51937.5703	p	CCD	−10449.0	−0.0010	Agerer & Hubscher (2002)
51950.4944	s	CCD	−9818.0	−0.0004	Agerer & Hubscher (2002)
52274.5538	p	CCD	−9791.5	−0.0013	Csizmadia et al. (2002)
52274.5955	p	CCD	−9127.0	−0.0021	*O–C* gateway[a]
52322.3948	p	Pe	−9029.0	−0.0011	Agerer & Hubscher (2003)
52337.5143	p	CCD	−8998.0	−0.0014	Agerer & Hubscher (2002)

Table 4
(Continued)

Epoch 2400000+	Type	Method	Epoch	*O–C*	References
52353.1189	p	CCD	−8966.0	−0.0045	*O–C* gateway[a]
52664.2967	p	CCD	−8328.0	−0.0035	*O–C* gateway[a]
52680.3927	p	Pe	−8295.0	−0.0028	Hubscher (2005)
52692.5878	p	CCD	−8270.0	−0.0012	Kotkova & Wolf (2006)
52705.7566	p	CCD	−8243.0	−0.0013	Nelson (2004)
52721.3633	p	Pe	−8211.0	−0.0022	Agerer & Hubscher (2003)
52721.6096	s	Pe	−8210.5	0.0002	Agerer & Hubscher (2003)
52983.2791	p	CCD	−7674.0	−0.0016	*O–C* gateway[a]
53001.3274	p	CCD	−7637.0	0.0003	*O–C* gateway[a]
53040.5894	s	CCD	−7556.5	−0.0006	Hubscher (2005)
53079.6099	s	CCD	−7476.5	0.0009	Hubscher (2005)
53359.8133	p	CCD	−6902.0	−0.0011	*O–C* gateway[a]
53379.5708	s	CCD	−6861.5	0.0030	Albayrak et al. (2005)
53381.5166	s	CCD	−6857.5	−0.0022	Hubscher et al. (2006)
53390.7818	s	CCD	−6838.5	−0.0040	Ogloza et al. (2008)
53409.5621	p	CCD	−6800.0	−0.0016	Hubscher et al. (2005)
53410.5389	p	CCD	−6798.0	−0.0003	Hubscher et al. (2005)
53421.2687	p	CCD	−6776.0	−0.0007	Kim et al. (2006)
53427.1211	p	CCD	−6764.0	−0.0012	Lee et al. (2006)
53428.0964	p	CCD	−6762.0	−0.0013	Lee et al. (2006)
53429.0720	p	CCD	−6760.0	−0.0012	Lee et al. (2006)
53432.9743	p	CCD	−6752.0	−0.0008	Lee et al. (2006)
53433.2180	s	CCD	−6751.5	−0.0010	Lee et al. (2006)
53445.4107	s	CCD	−6726.5	−0.0017	Hubscher et al. (2005)
53451.5041	p	CCD	−6714.0	−0.0050	Hubscher et al. (2005)
53461.0189	s	CCD	−6694.5	−0.0011	Lee et al. (2006)
53683.6714	p	CCD	−6238.0	−0.0010	Hubscher et al. (2006)
53720.2512	p	CCD	−6163.0	−0.0015	*O–C* gateway[a]
53749.5140	p	CCD	−6103.0	−0.0030	Hubscher (2007)
53814.3850	p	CCD	−5970.0	−0.0012	Hubscher et al. (2006)
53826.3363	s	CCD	−5945.5	0.0006	Senavci et al. (2007)
54086.5432	p	CCD	−5412.0	−0.0007	Dogru et al. (2009)
54097.2729	p	CCD	−5390.0	−0.0012	*O–C* gateway[a]
54149.4622	p	CCD	−5283.0	0.0001	Hubscher et al. (2009)
54174.3357	p	CCD	−5232.0	−0.0010	*O–C* gateway[a]
54174.5850	s	CCD	−5231.5	0.0044	Dogru et al. (2009)
54199.4560	s	CCD	−5180.5	0.0008	Dogru et al. (2009)
54193.3567	p	CCD	−5193.0	−0.0018	*O–C* gateway[a]
54499.4135	s	CCD	−4565.5	−0.0006	Yilmaz et al. (2009)
54509.4123	p	CCD	−4545.0	−0.0004	Hubscher et al. (2010)
54527.7025	s	CCD	−4507.5	−0.0004	Nelson (2009)
54531.3591	p	CCD	−4500.0	−0.0018	Hubscher et al. (2009)
54531.6054	s	CCD	−4499.5	0.0006	Hubscher et al. (2009)
54828.6380	s	CCD	−3890.5	0.0009	*O–C* gateway[a]
54831.5634	s	CCD	−3884.5	−0.0002	Hubscher et al. (2010)
54860.8268	s	CCD	−3824.5	−0.0011	Diethelm (2009)
54908.3830	p	CCD	−3727.0	0.0007	Hubscher et al. (2010)
55243.7032	s	CCD	−3039.5	0.0011	Diethelm (2010)
55269.3100	p	CCD	−2987.0	0.0016	*O–C* gateway[a]
55277.1126	p	CCD	−2971.0	0.0004	*O–C* gateway[a]
55297.3567	s	CCD	−2929.5	0.0034	*O–C* gateway[a]
55297.3587	s	CCD	−2929.5	0.0054	*O–C* gateway[a]
55534.6384	p	CCD	−2443.0	0.0006	*O–C* gateway[a]
55589.2655	p	CCD	−2331.0	0.0011	*O–C* gateway[a]
55601.4597	p	CCD	−2306.0	0.0018	Arena et al. (2011)
55649.7451	p	CCD	−2207.0	0.0012	Diethelm (2011)
55945.8032	p	CCD	−1600.0	0.0024	Nelson (2013)
55952.8778	s	CCD	−1585.5	0.0048	Diethelm (2012)
55959.2161	s	CCD	−1572.5	0.0025	*O–C* gateway[a]
55961.1672	s	CCD	−1568.5	0.0026	*O–C* gateway[a]
56018.7197	s	CCD	−1450.5	0.0020	Diethelm (2012)

Table 4
(Continued)

Epoch 2400000+	Type	Method	Epoch	*O–C*	References
56003.3569	p	CCD	−1482.0	0.0030	*O–C* gateway[a]
56400.3729	p	CCD	−668.0	0.0003	*O–C* gateway[a]
56713.0162	p	CCD	−27.0	0.0036	This Paper
56713.2607	s	CCD	−26.5	0.0043	This Paper
56716.1867	s	CCD	−20.5	0.0038	This Paper
56726.1872	p	CCD	0.0	0.0057	This Paper

Note. *O–C* gateway.
[a] http://var.astro.cz/ocgate/

the available literature and the database *O–C* gateway (http://var.astro.cz/ocgate/).

Adding the four times of minimum light in this paper, 234 times of minimum light have been collected, in which 72 are visual, 35 photograph, and 128 photoelectric (Pe) and CCD. The Pe and CCD times of minimum light for XZ Leo are listed in Table 4, where the second column shows the types of eclipses, and the notation p and s refers to the primary and the secondary minima, respectively. The third column shows the observation method. The corresponding epoch and *O–C* values are listed in the fourth and fifth columns based on the linear ephemeris

$$\text{Min. I} = 2456726.1706(7) + 0^{\text{d}}.48773679(4) \times E. \quad (1)$$

Then, together with all of the eclipse time data, the following quadratic ephemeris was derived using the least-squares method:

$$\text{Min. I} = 2456726.1863(4) + 0^{\text{d}}.48773918(5) \times E + 5.44 \times 10^{-11} \times E^2. \quad (2)$$

The *O–C* fit curves for XZ Leo are plotted in the upper panel of Figure 5 with solid lines. The observational data are plotted with open circles (photoelectric and CCD data), triangles (visual data), and plus signs (photographic data). Based on this ephemeris, a continuous period increase rate $dP/dt = +8.15 \times 10^{-8}$ days yr^{-1} was derived. This results is close to that of Lee et al. (2006), $dP/dt = +8.20 \times 10^{-8}$ days yr^{-1}. The residuals based on the ephemeris (Equation (2)) are plotted in the lower panel of Figure 5, where no significant systematic variation can be traced. When considering only the photoelectric and CCD times of minimum light, we can obtain another quadratic ephemeris with the same method,

$$\text{Min. I} = 2456726.1851(2) + 0^{\text{d}}.48773886(5) \times E + 4.08 \times 10^{-11} \times E^2. \quad (3)$$

A continuous period increase can be clearly seen in the upper panel of Figure 6 (solid line). A period increase rate of $dP/dt = +6.12 \times 10^{-8}$ days yr^{-1} was obtained, which is slightly smaller than that derived from all of the minimum data (Equation (3)). The resulting residuals based on Equation (4) are plotted in the bottom panel of Figure 6 where no systematic deviations are evident. The orbital period's increase during the contact phase can be interpreted as conservative mass transfer from the less massive component to the more massive one. The parameters of the system (e.g., the orbital period, the mass ratio, the degree of contact) are changing on the thermal timescales of the components. The contact binary must undergo cycles around the state of marginal contact, and it will evolve into a broken-contact binary at last, as predicted TRO theory (Flannery 1976; Lucy 1976; Robertson & Eggleton 1977). Therefore, XZ Leo should evolve to the broken-contact phase as suggested by Qian (2001b). Based on mass and angular momentum conservation and the equivalent radius of the

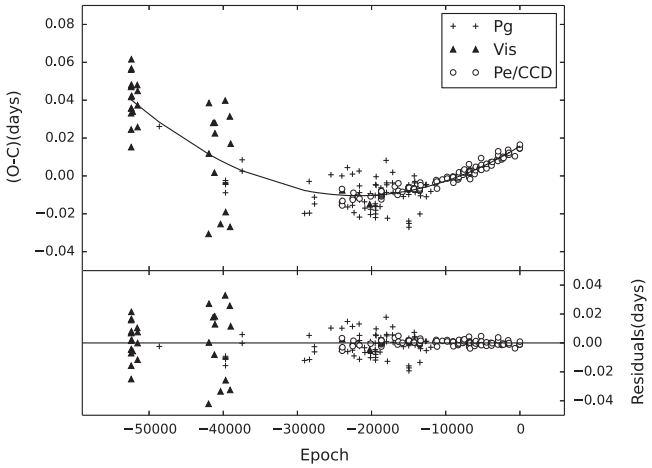

Figure 5. *O–C* curve of contact binary XZ Leo with all of the observation data. Upper panel: *O–C* diagram computed with Equation (3) with the solid line, indicating that there is a long-term period increase. Bottom panel: resulting residuals. Open circles denote CCD and photoelectric data, triangles denote the photographic data, and plus signs the visual data.

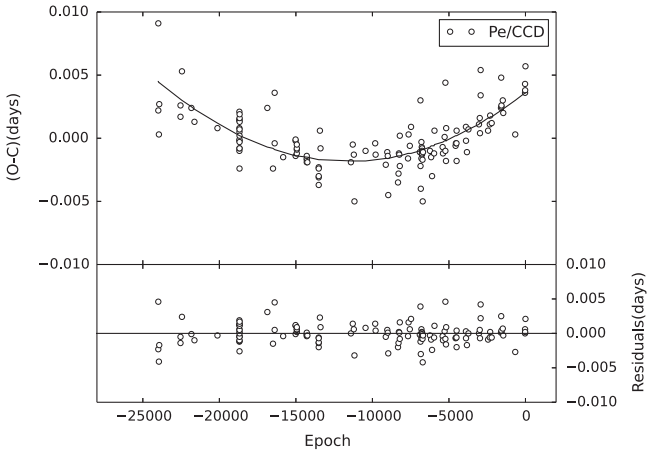

Figure 6. *O–C* curves of XZ Leo with only photoelectric and CCD data.

Table 5
Absolute Parameters of XZ Leo

Parameter	Primary	Secondary
$M(M_\odot)$	1.74(6)	0.61(2)
$R(R_\odot)$	1.69(1)	1.07(1)
$L(L_\odot)$	6.73(8)	2.40(4)

Roche Lobe, we estimated the evolution time of XZ Leo from contact to broken-contact status. The equivalent radius of the Roche Lobe could be written as $R_{cr2} = r_{cr2}A$, and

$$r_{cr2} = \frac{0.49q^{2/3}}{0.6q^{2/3} + 1n\left(1 + q^{1/3}\right)} \quad (4)$$

following Eggleton (1983), where q is the mass ratio ($q = M_2/M_1$) and A is the distance between two components. We conclude that this contact binary will evolve to broken-contact phase in 1.56×10^6 years. A corresponding 0.06 $M_\odot$ will be transfered from the secondary to the primary component and the mass ratio will be decreased to 0.304.

5. DISCUSSIONS AND CONCLUSIONS

We have presented *VRI* band time-series CCD photometry of the contact binary XZ Leo. The light curve of this system has a long-lived asymmetric phenomenon in the placement of the light maxima from Hoffmann (1984), to Lee et al. (2006), to this paper. This long-lived phenomenon may be caused by mass transfer through the neck region. Moreover, this system has a continuous period increase (Qian 2001a; Lee et al. 2006), with mass transfer from the secondary component (less massive) to the primary component (more massive). A hot spot could be caused by the gas streams from the secondary component that impact the inner hemisphere of the primary component. Therefore, a hot spot was introduced in our theoretical light curve. Based on our new light curves of XZ Leo and the published radial-velocity data (Rucinski & Lu 1999), we carried out a detailed light curve analysis for this system using the W–D code. A good fit to the observations was obtained with binary mode 3 under a hot spot on the primary component near the neck region of the common envelope. The photometric solutions reveal that XZ Leo is an A-type system with a degree of contact of $f = 24(\pm1)\%$. The effective temperatures of the components show that it is a hot contact binary with a small difference in temperature of $\Delta(T_1 - T_2) = 179$ K. By combining our photometric solutions with radial-velocity curves derived by Rucinski & Lu (1999), the absolute parameters of XZ Leo were computed and the results are listed in Table 5.

To investigate the period variations of XZ Leo, all available times of minimum light were collected. Finally, 234 times of minimum light were selected, where 128 came from the photoelectric and CCD observation. By combining our new times of minimum light with all available timings, the new *O–C* diagrams of XZ Leo were analyzed, and reveal that the period of XZ Leo is increasing continuously at a rate of $dP/dt = +8.15 \times 10^{-8}$ days yr^{-1} with all of the data. To obtain a more accurate period change, we used only the photoelectric and CCD data with the same method. A continuous period increase of dP/dt was also presented and a period increase rate of $dP/dt = +6.12 \times 10^{-8}$ days yr^{-1} was obtained, which is slightly smaller than that derived from all existing data. The continuous period increase can be explained by mass transfer from the secondary (the less massive component) to the primary component (the more massive component), which is in agreement with the predictions of TRO theory. The TRO theory suggests that the evolution of W UMa stars must undergo oscillations around the status of contact and non-contact. This indicates that the contact binary XZ Leo is in an expanding TRO state before the broken-contact phase at present, as suggested by Qian (2001a). By considering conservative mass transfer, a calculation with the well-known equation

$$\dot{P}/P = -3\dot{M}_2\left(1/M_1 - 1/M_2\right) \quad (5)$$

leads to a mass transfer rate of $dM_2/dt = 3.92 \times 10^{-8} M_\odot$ yr^{-1}. This will cause the mass of the secondary component and hence the mass ratio to decrease. Conclusively, the contact binary of XZ Leo will evolve to broken-contact state. Based on mass and angular momentum conservations, the time of evolution from contact to broken-contact state was estimated to be 1.56×10^6 years. About 0.06 $M_\odot$ will be transfered from the secondary to the primary component and the mass ratio q will decrease from 0.348 to 0.304.

This work is supported by the National Natural Science Foundation of China (NSFC) and the NSFC/CAS Joint Fund of Astronomy through grants 11373037, 11303021, U1231202, and 2013CB834900. L.D. acknowledges partial support by the National Key Basic Research Program of China 2014CB845703. The authors are grateful to the anonymous referee for valuable comments.

REFERENCES

Agerer, F., & Hubscher, J. 1996, IBVS, 4383, 1
Agerer, F., & Hubscher, J. 1997, IBVS, 4472, 1
Agerer, F., & Hubscher, J. 1999, IBVS, 4711, 1
Agerer, F., & Hubscher, J. 2000, IBVS, 4912, 1
Agerer, F., & Hubscher, J. 2002, IBVS, 5296, 1
Agerer, F., & Hubscher, J. 2003, IBVS, 5484, 1
Albayrak, B., Yuce, K., Selam, S. O., et al. 2005, IBVS, 5649, 1
Arena, C., Aceti, P., Banfi, M., et al. 2011, IBVS, 5997, 1
Braune, W., & Mundry, E. 1982, BAV Mitt, 34
Csizmadia, S., Zhou, A. Y., Konyves, V., et al. 2002, IBVS, 5230, 1
Diethelm, R. 1992, BBSAG Bull, 100
Diethelm, R. 1995, BBSAG Bull, 108
Diethelm, R. 2009, IBVS, 5894, 1
Diethelm, R. 2010, IBVS, 5945, 1
Diethelm, R. 2011, IBVS, 5992, 1
Diethelm, R. 2012, IBVS, 6029, 1
Dogru, S. S., Erdem, A., & Donmez, A. 2009, IBVS, 5893, 1
Eggleton, P. P. 1983, ApJ, 268, 368
Faulkner, D. R. 1986, PASP, 98, 690
Flannery, B. P. 1976, ApJ, 205, 317
Flower, P. J. 1996, ApJ, 469, 355
Hoffmann, M. 1983, IBVS, 2344, 1
Hoffmann, M. 1984, Veroff. Astr. Instr. Bonn, 96
Hoffmeister, C. 1934, AN, 253, 195
Harmanec, P. 1988, Astron. Inst. Czech, 39, 329
Hubscher, J. 2005, IBVS, 5643, 1
Hubscher, J. 2007, IBVS, 5802, 1
Hubscher, J., Agerer, F., & Wunder, E. 1992, BAV Mitt, 60
Hubscher, J., Agerer, F., & Wunder, E. 1993, BAV Mitt, 62
Hubscher, J., Agerer, F., & Wunder, E. 1994, BAV Mitt, 68
Hubscher, J., Lehmann, P. B., Monninger, G., et al. 2010, IBVS, 5918, 1
Hubscher, J., Lichtenknecker, D., & Munder, E. 1985, BAV Mitt, 39
Hubscher, J., Lichtenknecker, D., & Wunder, E. 1989, BAV Mitt, 52
Hubscher, J., & Mundry, E. 1984, BAV Mitt, 38

Hubscher, J., Paschke, A., & Walter, F. 2005, IBVS, 5657, 1
Hubscher, J., Paschke, A., & Walter, F. 2006, IBVS, 5731, 1
Hubscher, J., Steinbach, H.-M., & Walter, F. 2009, IBVS, 5874, 1
Keskin, V., & Pohl, E. 1989, IBVS, 3355, 1
Kim, C.-H., Lee, C.-U., Yoon, Y.-N., et al. 2006, IBVS, 569
Kotkova, L., & Wolf, M. 2006, IBVS, 5676, 1
Kwee, K. K., & van Woerden, H. 1956, BAN, 12, 327
Lee, J. W., Lee, C.-U., Kim, C.-H., & Kang, Y. W. 2006, JKAS, 39, 41
Lucy, L. B. 1967, ZA, 65, 89
Lucy, L. B. 1976, ApJ, 205, 208
Niarchos, P. G., Hoffmann, M., & Duerbeck, H. W. 1994, A&A, 292, 494
Nelson, R. H. 2001, IBVS, 5040, 1
Nelson, R. H. 2004, IBVS, 5493, 1
Nelson, R. H. 2009, IBVS, 5875, 1
Nelson, R. H. 2013, IBVS, 6050, 1
Ogloza, W., Niewiadomski, W., Barnacka, A., et al. 2008, IBVS, 5843, 1
Prichodko, A. 1947, Variable Stars, 6, 135
Qian, S. B. 2001a, MNRAS, 328, 914
Qian, S. B. 2001b, MNRAS, 328, 635
Qian, S. B. 2003, MNRAS, 342, 1260
Robertson, J. A., & Eggleton, P. P. 1977, MNRAS, 179, 359
Rucinski, S. M. 1969, AcA, 19, 245
Rucinski, S. M., & Lu, W. 1999, AJ, 118, 2451
Senavci, H. V., Tanriverdi, T., Torun, E., et al. 2007, IBVS, 5754, 1
Yilmaz, M., Basturk, O., Alan, N., et al. 2009, IBVS, 5887, 1
van Hamme, W. 1993, AJ, 106, 2096
Wilson, R. E. 1979, ApJ, 234, 1054
Wilson, R. E. 1990, ApJ, 356, 613
Wilson, R. E. 1994, PASP, 106, 921
Wilson, R. E., & Devinney, E. J. 1971, ApJ, 166, 605
Wilson, R. E., & van Hamme, W. 2003, Computing Binary Stars Observables (W-D Program, 4th ed.), ftp://ftp.astro.ufl.edu/pub/wilson/lcdc2003
Wunder, E., Wieck, M., Kilinc, B., et al. 1992, IBVS, 3760, 1
Zhou, A. Y., Jiang, X. J., Zhang, Y. P., & Wei, J. Y. 2009, RAA, 9, 349